OPEN ACCESS

GAVIN PUBLISHERS

International Journal of Pollution Research

Hiluf H, et al. Int J Pollut Res: IJPR-109.

Research Article

DOI: 10.29011/IJPR -109.100009

Photo-Catalytic Degradation of Phenol Red Dye from Contaminated Water Over Nanosize Tio_2, N-Doped-Tio_2, Tio_2/WO_3 and N-Doped Tio_2/WO_3

Hayelom Hiluf, Om Prakash Yadav*, Abi M. Taddesse

Department of Chemistry, Haramaya University, Post Box: 138, Dire Dawa, Ethiopia

***Corresponding Author:** Om Prakash Yadav, Department of Chemistry, Haramaya University, Post Box 138, Dire Dawa, Ethiopia. Tel: +918059602660; Email: yadavop02@yahoo.com

Citation: Hiluf H, Yadav OP, Taddesse AM (2019) Photo-Catalytic Degradation of Phenol Red Dye from Contaminated Water Over Nanosize Tio2, N-Doped-Tio2, Tio2/WO3 and N-Doped Tio2/WO3. Int J Pollut Res: IJPR-109. DOI: 10.29011/IJPR -109.100009

Received Date: 22 August, 2019; **Accepted Date:** 28 October, 2019; **Published Date:** 01 November, 2019

Abstract

Nano size TiO_2, N-doped TiO_2, TiO_2/WO_3 and N-doped TiO_2/WO_3 composite semiconductor photo-catalysts powders were prepared following sol-gel and solid phase reaction techniques and characterized using XRD, SEM, EDS and UV-Visible spectroscopic techniques. As revealed from X-ray diffraction analysis, the crystallite size of synthesized material was within 9 to 12 nm. XRD patterns revealed that TiO_2 powder existed in anatase as well as rutile phases, while WO_3 existed in monoclinic form. UV-visible diffuse absorption spectra indicated that absorption edge of N-doped TiO_2, TiO_2/WO_3 and N-doped TiO_2/WO_3 well extends to visible region compared to pure TiO_2. Photo-catalytic activities of as-synthesized nanoparticles were compared using degradation of phenol red dye, as a probe. Doping of nitrogen and compositing WO_3 with TiO_2 both had synergetic effect towards improving the photo-catalytic activity of TiO_2. Using N-doped TiO_2/WO_3 photo-catalyst, phenol red in its 50 mgL^{-1} solution with photo-catalyst load 150 mgL^{-1} could be degraded up to 74.7 and 92.6 %, under UV and solar radiation, respectively. The results show that the above composite photo-catalyst may be recommended for low-cost and efficient treatment of bulk or effluent water contaminated with phenol red, using solar radiation.

Keywords: Degradation; EDS; Nanoparticles; Phenol Red; Photo-Catalytic

Introduction

Effluents from paper, textile and dyeing industries and petroleum refineries are contaminated with organic pollutants such as dyes, phenols and hydrocarbons. These chemicals and their metabolites being toxic and non-biodegradable in nature cause serious environmental pollution impacting human health as well as eco-system [1]. For example, nitro aromatic compounds exhibit high toxicity and/or mutagenicity for living organisms either directly or through some of their catabolic metabolites [2]. The usual physical, chemical. and biological methods adopted for the removal of organic pollutants from contaminated water are inefficient and generate a large amount of sludge as a solid waste that requires secondary treatment. Advanced oxidative photo-catalytic degradation of organic pollutants in water and air may provide an excellent solution for environmental cleanup without generating toxic byproducts as this technique enables complete oxidation of the pollutants and their conversion to benign species. Absorption of a photon of wavelength adequate to band gap energy (E_g) of the semiconductor photo-catalyst results in the promotion of an electron from its Valence Band (VB) to Conduction Band (CB) creating a hole (h^+) at the VB. The photo-generated electron/hole pair can either recombine releasing energy as heat or these charge carriers migrate to the photo-catalyst's surface. Whereas, the photo-excited electrons at the CB reacts with surface adsorbed oxygen, the holes at the VB interact with water molecule forming highly reactive hydroxyl radicals that enable degradation of organic pollutant molecules forming CO_2, H_2O, and simple non-toxic end products.

The researchers in this area have mainly focused on understanding the fundamentals of photo-catalytic processes and to explore the possible means of improving efficiencies of high band gap photo-catalysts in the visible region of radiation in order to harvest the freely available solar energy thus making the process cost effective [3-6]. Nano-size (1-100 nm) semiconductor particles due to their large specific surface areas have great potential as water and air purifier as these can provide redox active media. Besides it, the nanoparticles can also exhibit their size and shape-dependent optical, electronic and catalytic properties [7].

Though a wide range of semiconductor material may be used in photo-catalytic degradation reactions, yet an ideal photo-catalyst should be chemically inert, stable toward photo-corrosion, non-toxic, photoactive under visible light and of low-cost [8]. Titanium dioxide (TiO_2) has been used in glass manufacturing,

electro ceramics, self-cleaning surfaces and as a photo-catalyst, under UV irradiation, for photo degradation of numerous organic pollutants in water and air [9-11]. It may be due to its high ultraviolet absorption, biological and chemical inertness, cost effectiveness, non-toxicity, and long-term stability against chemical corrosion.

Reza, et al. [12] has reviewed the parameters affecting photo-catalytic degradation of dyes using TiO_2. Due to the large band gap of TiO_2, its photo-excitation requires high energy UV radiation and its catalytic efficiency is low in solar radiation. A higher rate of electron-hole recombination in photo-excited TiO_2 also reduces its catalytic efficiency. In addition to these drawbacks, high cost of UV source, required for the photo-excitation, the use of TO_2, as a catalyst for a large scale treatment of water may not be economical. Therefore, this has prompted the researchers for further studies to improve photo-catalytic efficiency of high band gap photo-catalysts under visible radiation. Such studies mostly involve modification of the photo-catalysts by doping metals/ non-metals or by adopting surface-complex-mediated path [13-19].

Another approach for improving the photo-catalytic efficiency of high band gap energy (E_g) semiconductors could be by mixing these with a low band gap semiconductor. According to the inter-particle electron-transfer theory, visible light can photo-excite a low band gap semiconductor which in turn can photosensitize another semiconductor with high electrical potential and large band gap resulting in the enhanced photo-catalytic reaction. Sant & Kamat [20] investigated inter-particle electron transfer between size-quantized CdS and TiO_2 semiconductor nanoclusters. They have found that electron transfer from low band gap photo excited CdS (E_g = 2.4 eV) to high band gap TiO_2 (E_g = 3.2 eV) depends on the particle size of TiO_2 charge and the transfer was observed only when TiO_2 particles were sufficiently large (>12 Å). However, according to Tian, et al. [21], coupling of TiO_2 with another semiconductor with lower band gap energy such as WO_3 (E_g =2,7 eV) to serve as an electron accepter, can improve the photo-catalytic properties of TiO_2. As a basic function, WO_3 has a suitable conduction band potentially to allow the transfer of photo-generated electrons from TiO_2 facilitating effective charge separation. In addition to this, formation of a monolayer of WOx species on TiO_2 can significantly increase the surface acidity [22,23]. Owing to such enhanced acidity, TiO_2/WO_3 can absorb more hydroxyl groups and simultaneously more organic reactants on its surface resulting in an improvement of the photocatalytic activity vis-à-vis the pure TiO_2 photo-catalyst. Boga et al. [24] from spectroscopic and structural analysis of TiO_2/WO_3 have reported that due to higher charge separation efficiency and the surface hydrophilicity, the above composite photo-catalyst can enhance the photo-catalytic degradation of oxalic acid under UV light in aqueous media.

However, no reports have appeared on the photo-catalytic activity of TiO_2/WO_3 or N-doped TiO_2/WO_3 composite photo-catalysts for photo-degradation of phenol red-an organic pollutant in contaminated water. Phenol red exists as a red crystal that is stable in air and has solubility 0.77 g L^{-1} in water. It exhibits a gradual transition in color from yellow (λ_{max} = 443 nm) to red (λ_{max} = 570 nm) over the pH range 6.8 to 8.2. Phenol Red (PR) also known as phenol sulfonaphthalein is a pH indicator and frequently used in cell biological laboratories for determining kidney function, is toxic in nature. On contact with eye and skin, it causes irritation and if inhaled, it is harmful for respiratory tract and digestive system. This paper reports a comparative photo-catalytic degradation of phenol red in aqueous medium using sol-gel and hydrothermally synthesized and duly characterized Nano size TiO_2, N-doped-TiO_2, TiO_2/WO_3 and N-doped TiO_2/WO_3 composites as photo-catalysts.

Materials and Methods

Chemicals

Titanium tetrachloride $TiCl_4$ (MW 189.87 g.mol^{-1}, 99.9%; SD chemicals); TiO_2 (Degussa p-25, MW: 79.9 g.mol^{-1}, 99%, Germany); WO_3 (MW 231.84 g.mol^{-1}, 99%, SD fine chemicals,); Ethanol, C_2H_3OH (MW 58.03 g.mol^{-1}, 99.9%, Park scientific); Ammonium hydroxide, NH_4OH (MW 35.04 g.mol^{-1}, Abron chemicals); Urea (MW 60.06 g.mol^{-1}, extra pure BLULUX)) and Phenol Red ($C_{19}H_{14}O_5S$, MW: 354.38 g·mol^{-1}, BLULUX) were of analytical grade. Molecular structure of Phenol Red is shown in Figure 1.

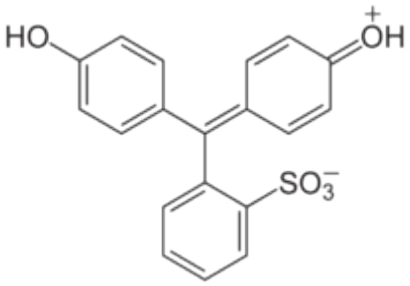

Figure 1: Molecular structure of Phenol- red (phenolsulfonphthalein).

Methods

Preparation of TiO_2 Nanoparticles

Nano Size Titanium Dioxide (TiO_2) was prepared by following sol-gel route [25,26]. The precursor titanium tetrachloride ($TiCl_4$) was added to distilled water taken in a glass conical flask, kept in an ice bath. To this, ethanol and ammonium hydroxide solution were mixed with vigorous stirring for 30 min. The precipitate thus obtained was thoroughly washed with distilled water for the removal of chloride ions, dried at 110 ˚C. The product was calcinated at 400 ˚C. for four hours, cooled and ground to get a fine powder

Preparation of N-doped TiO_2

Nitrogen doped TiO_2 nanoparticles were prepared by solid phase reaction method, described elsewhere [26]. Typically, urea and as-synthesized TiO_2 with molar ratio = 1:3, were mixed in a ceramic crucible and calcinated at 400 ˚C for 4 hrs. The product was cooled to room temperature, crushed to get fine powder and then stored in a moisture-free atmosphere before further use.

Preparation of WO_3 coupled TiO_2

As-synthesized TiO_2 and WO_3 (molar ratio 95: 5) were thoroughly mixed with equimolar mixture of ethanol and water [27], dried at 110 ˚C and calcinated at 400 ˚C for four hrs. The product was then cooled and crushed to a fine powder.

Preparation of N-doped TiO_2/WO_3

As-synthesized N-doped TiO_2 and WO_3 (95:5, w/w) were thoroughly mixed in an equimolar mixture of ethanol and water. The mixture was dried up at 110 ˚C for 2 h and then calcinated at 400 ˚C for 4h. The product was crushed to fine powder at room temperature before further use.

XRD Analysis

XRD patterns of as-prepared photo-catalysts powders were obtained over 2θ range: 20-60˚ using an X-Ray Diffractometer (Bruker D8 Advance XRD) and Cu Kα radiation (λ = 0.154056 nm). The X-ray diffractometer was operated at 40 kV and 40 mA under scan rate 0.02˚ min^{-1}

SEM Analysis

A drop of photo-catalyst powder dispersion in acetone was released over the carbon SEM stub. The stub was then heated in a vacuum oven for 10 min at 200 ˚C and subsequently cooled to room temperature. The SEM image of each sample was obtained using accelerating voltage 15 kV at different magnifications.

UV/Visible Analysis

For determining photo absorption edge and band gap energy of photo-catalyst powders, optical absorbance of their aqueous suspension (0.01%, w/v) were recorded over 200-800 nm using a UV/Visible spectrophotometer (JASCOV 550).

Photocatalytic Degradation Study

Photo-catalytic degradation of Phenol-Red (PR) was carried out using a batch type reactor, described, elsewhere [28]. It comprised of a quartz tube with an effective volume of 250 mL and provided with an inlet for air-purging and an outlet for the collection of reaction mixture. Each time, 100 mL PR aqueous solution of specified initial concentration (pH =6.7) mixed with a known amount of photo-catalyst powder was taken in the reactor tube and stirred in dark for an hour to achieve sorption-desorption equilibrium between photo-catalyst powder and PR solution. A UV lamp (12W, Philips) emitting radiation at 254 nm and operated at 230 Volts and 50 Hz, was used as a UV source. The lamp was kept at 12 cm above the top of the reactor tube. Exposure of PR solution to the solar radiation was done on clear days, during 10 AM to 4 PM. at Haramaya University, Ethiopia ($9^0$25'30" N & $42^0$2'0"E). During irradiation, the reaction mixture was purged with air at flow rate 100 ml L^{-1}. A five mL each of reaction mixture was collected at a regular interval, centrifuged at 4000 rpm for 5 minutes and filtered through a 0.5 µm pore size membrane. Absorbance of the filtrate was recorded at 432 nm on a spectrophotometer (JASCOV 550) and the percent degradation of the substrate (PR) was calculated using the relation-

$$\% \text{ Degradation} = [(A_o - A_t)/A_o] \times 100 \quad (1)$$

Where, A_o and A_t are absorbance values at initial stage of reaction and at time 't', respectively.

Results and Discussion

XRD Analysis

XRD patterns of as-synthesized photo-catalysts: TiO_2, N-doped TiO_2, TiO_2, /WO_3 and N-doped TiO_2, /WO_3 are presented in Figure 2. The XRD of TiO_2 powder calcinated at 400 ˚C showing diffraction peaks at 2θ = 25.5, 38.7, 48.2, 54.9 and 64.0˚ corresponding to the crystal planes (101), (004), (200), (105) and (204), respectively, revealed the existence of tetragonal anatase phase of TiO_2 in agreement with the standard spectrum (JCPDS Card Nos. 21-1272). However, the reflections at 27.0, 56.6 and 69.4˚ from the crystal planes (110), (220) and (301) also indicated the presence of some rutile phase [JCPDS 84-1286)] as well in the synthesized TiO_2 powder. The observed XRD pattern for N-doped TiO_2 was similar to that of calcinated TiO_2 suggesting that crystal structure of the later is unaltered by the doped nitrogen. Since no additional diffraction peak is observed in the XRD pattern of N-doped TiO_2 vis-à-vis TIO_2, it suggests that the anatase and rutile phases of TiO_2 remain intact on doping N. It also implies that the guest N atoms in the crystal lattice are distributed substituting equal number of oxygen atoms [29]. Further, in the XRD patterns of TiO_2/WO_3 and N-TiO_2/WO_{3s} composites, the observed low intensity additional peaks at 25.0, 28.1, 35.2, 37.9 and 52.0 are from (110), (200), (111), (201) and (220), respectively, planes of WO_3 hexagonal phase (JCPDS Card No. 033-1387) and the peaks pattern suggests the compositing WO_3 with TiO_2 results in shifting of anatase ⇌ rutile equilibrium in favor of rutile phase.

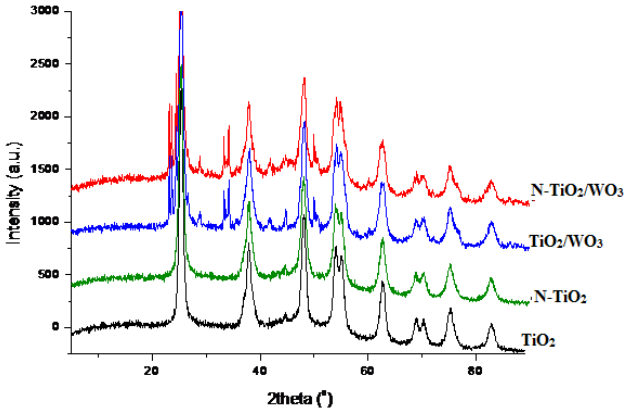

Figure 2: XRD Patterns of as-synthesized TiO_2, N-doped TiO_2, TiO_2/WO_3 and N-doped TiO_2/WO_3 photo-catalysts powders.

The average crystallite size of as-synthesized photo-catalysts powders were obtained using Dubye Scherrer equation-

$$D = K.\lambda / (\beta.\cos\theta) \quad (2)$$

Where, D is crystallite size in nanometer, K is shape factor constant equal to 0.9, β is the full width at half maximum (FWHM) in radians of the most intense diffraction peak, λ is the X-ray wave length (0.15406 nm) and θ is Bragg's angle. Average crystallite size, diffraction angle (2θ) of most intense diffraction peak and β values are given in Table 1. Average crystallite size of synthesized photo-catalyst powders were in the range 9-12 nm

Photo-catalyst	2θ (degree)	β (radian)	D (nm)
TiO_2	25.59	0.0120	11.9
N-TiO_2	25.42	0.0147	9.7
TiO_2/WO_3	25.45	0.0156	9.2
N-TiO_2/WO_3	25.59	0.0133	10.6

Table 1: Diffraction angle (2θ) and β (full width at half maximum FWHM) of the most intense diffraction peak and crystallite size (D) for synthesized photo-catalyst powders.

SEM Analysis

Scanning Electron Microscopic (SEM) images for photo-catalysts powders using accelerating voltage 15 kV at similar magnification, are presented in Figure 3. Particles consisting of coherently scattered domain in the size range 5-50 nm are found to be agglomerated and of polycrystalline nature. The observed SEM images distinctly display the irregular shapes as well as size of the individual particles and the fine detail of surface topography. The observed diverse shaped SEM images included Nano platelet structure, with non-uniform size with thickness 60 to 300 nm and width/diameter 0.5 to 1.5 μm. Also in the SEM figures are nanorods-nanobelts 40-70 nm thick 10-15 μm long. In the SEM images, some urchin-like structures, with dimensions in the nanorange, were also observed. At identical magnification of SEM, average particle size of synthesized TiO_2/WO_3 or N- TiO_2/WO_3 composites is smaller compared to pure TiO_2 and N-doped TiO_2 photo-catalysts. This suggests that compositing WO_3 with TiO_2 not only promotes transforming anatase to rutile phase, described above, but can also prevents the growth of the catalyst crystallites.

Further, in SEM images of TiO_2/WO_3 or N-TiO_2/WO_3 composite photo-catalysts, WO_3 particles appear smaller in size and brighter in appearance compared to the TiO_2 particles. These features may be attributed to the larger atomic number of W (compared to Ti). As a basic principle, element with larger atomic number tends to agglomerate less resulting in its smaller size, but it appears brighter owing to more intense back-scattering of surface electrons.

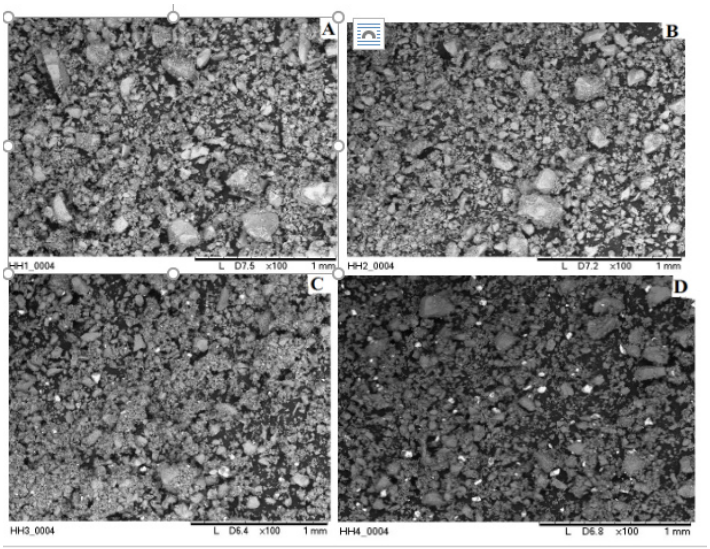

Figure 3: Scanning Electron Microscopic (SEM) images of synthesized photo-catalysts powders at accelerating voltage 15 kV. **(A)**: Calcined TiO_2, **(B):** N-doped TiO_2, **(C):** TiO_2/WO_3**, (D)**: N-TiO_2/WO_3.

EDS Analysis

The elemental distribution of synthesized photo-catalyst material was investigated using energy dispersive X-ray system (EDS). The EDS spectra of TiO_2, N-doped TiO_2, TiO_2/WO_3 and N-doped TiO_2/WO_3 are presented in Figure 4. In case of TiO_2 and N-doped TiO_2 photo-catalysts, only two peaks, one for oxygen and the other for titanium, are observed. However, the absence of nitrogen peak in case of N-doped TiO_2 EDS spectra may be due to the overlap of nitrogen (K) and Titanium (L) energy peaks. Whereas, in the TiO_2/WO_3 composite sample, Ti and W percent concentrations (w/w) were: 97.9 and 2.1, respectively, while for N-TiO_2/WO_3 these were 96.2 and 3.8%, respectively. Since no peak representing any other foreign element, within the detection limit of the EDS spectrometer, were detected, it also established the purity of as synthesized photo-catalyst samples.

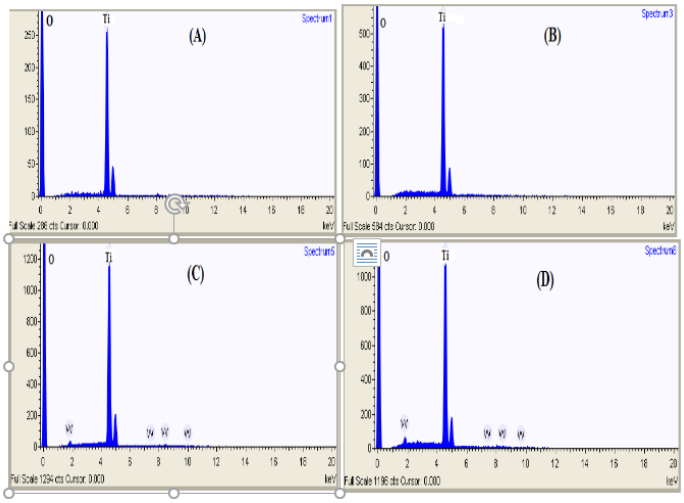

Figure 4: Energy Dispersive X-Ray Spectra (EDS) and elemental percent composition (w/w) (excluding N and O) **(A)**: TiO_2 [Ti =100 %]; **(B):** N-doped TiO_2, [Ti =100 %]; **(C):** TiO_2/WO_3 [Ti=97.9% and W=2.1%]; **(D)**: N-doped TiO_2/WO_3[Ti=96.2% and W=3.8%].

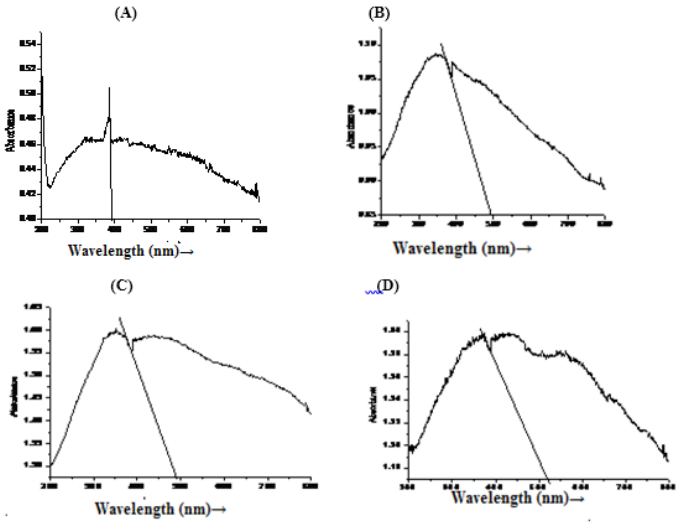

Figure 5: UV-Visible diffuse absorption spectra of synthesized photo-catalysts: **A** = TiO_2, **B** = N-doped TiO_2; **C**= TiO_2/WO_3 composite and **D**= N-doped TiO_2/WO_3 composite.

UV/Visible Spectroscopic Analysis

UV–Visible diffuse reflectance spectra of synthesized photo-catalyst powders dispersed in aqueous medium are presented in Figure 5. Absorption edges of TiO_2, N-doped TiO_2, TiO_2/WO_3 and N-TiO_2/WO_3 composites were 397, 492, 485 and 520 nm, respectively. The observed red shift of absorption edge from 397 nm to 495 nm on doping N in TiO_2 may be due to the incorporation of 2p energy levels of N within the valence and conduction bands of TiO_2 causing band gap narrowing. The observed absorption edge shifting to higher wavelength in case of N-doped TiO_2 also ensures successful doping of N into TiO_2. Absorption wavelength of TiO_2/WO_3 composite is also well extended to higher wave length (485 nm) vis-à-vis TiO_2 (397 nm). This may be attributed to the intermixing of energy levels of the two photo-catalysts leading to the lowering of band gaps. Highest observed absorption wave length (520 nm) in case of N-doped TiO_2/WO_3 composite, among the studied photo-catalysts, may be due to cumulative synergetic effect of band gap narrowing caused due to N-doping as well as compositing the two photo-catalysts.

Band gap energy of photo-catalysts were calculated using the relation-

$$E_g = 1240/\lambda \qquad (3)$$

Where, E_g is band gap energy in electron volts, and λ is the absorption edge wavelength (nm).

The band gap energy thus calculated for TiO_2, N-doped TiO_2, TiO_2/WO_3 and N-TiO_2/WO_3, are: 3.12, 2.52, 2.56 and 2.38 eV, respectively.

Photo-Catalytic Degradation Study

Plots of percent photo-catalytic degradation of Phenol Red (PR) over different photo-catalysts as a function of time, using substrate initial concentration, 50 mgL^{-1} and photo-catalyst load 150 mgL^{-1}, under UV and solar radiations are presented in Figure 6 and Figure 7, respectively. Phenol red degradation at three hrs. Over uncalcined TiO_2, calcined TiO_2, Degussa p-25, N-doped TiO_2, TiO_2/WO_3 and N-doped TiO_2/WO_3 under UV radiation were: 1.39, 28.6, 37.9, 40.3, 68.7 and 74.7 %, respectively and under solar radiation were: 1.4, 54.3, 56.4, 83.3, 85.2 and 92.6, respectively. Percent degradation values of PR at 3 hrs. using its initial concentration 50 mgL^{-1} and photo-catalyst load 150 $mgL^{-1}$are presented in Table 2. Photo-catalytic activity of Degussa P-25, was found to be higher compared to uncacined TiO_2 or calcined TiO_2 under UV as well as visible radiations. It may be because the Degussa P-25 mainly consists of photo-active anatase phase (60-70%) (along with less active minor amounts of rutile and other amorphous forms), whereas the uncalcined TiO_2 is a photo-inactive amorphous substance and calcinated TiO_2 may be having lesser proportion of anatage in the mixed phases than in Degussa P-25 [29]. Degradation of phenol red over N-doped TiO_2 was higher compared to Degussa P-25 and pure TiO_2 under solar radiation than under UV radiation. This may be attributed to the red-shift in photo-absorption enhancing photo response of N-doped TiO_2 in the visible region and a lowered rate of electron-hole recombination. The improved photo-catalytic performance under UV as well as solar radiations in case of coupled semiconductor system (TiO_2/WO_3) compared to pure TiO_2 can be attributed to synergetic effects

of enhanced charge separation efficiency as well the surface hydrophilicity in case of the composite semiconductors [30].

Since among the studied photo-catalysts, N-doped TiO_2/WO_3 composite could exhibit as high as 92.6% degradation of PR at 3 hrs using dye initial concentration 50 mgL^{-1} and photo-catalyst load 150 mgL^{-1} under solar radiation, this composite photo-catalyst can be recommended for a low cost and efficient treatment of bulk water or industrial effluent contaminated with phenol red.

Photo-Catalyst	% Degradation Under UV Radiation	% Degradation Under Solar Radiation
TiO_2(uncalcined)	1.40 ±01	1.42 ±0.01
TiO_2(calcinated)	28.62 ±0.03	54.32 ±0.05
P-25	37.86 ±0.06	56.41±0.06
N-TiO_2	40.34 ±0.15	83.26 ±0.12
TiO_2/WO_3	68.73 ±0.26	85.18 ±0.13
N-TiO_2/WO_3	74.71 ±0.42	92.57 ±0.15

Table 2: Percentage (%) Degradation of Phenol Red (PR) under UV and visible radiations at 3 hrs. (initial concentration of PR = 50 mg L^{-1}; Photo-catalyst load= 150 mgL^{-1}).

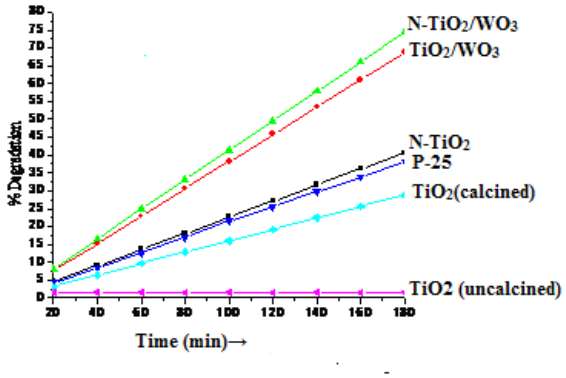

Figure 6: Percent degradation of Phenol Red (PR) under UV radiations as a function of time (initial concentration of PR = 50 mg L^{-1}; Photo-catalyst load= 150 mgL^{-1}).

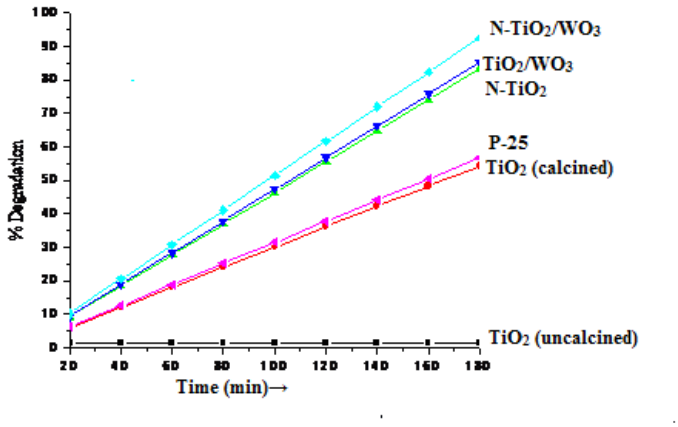

Figure 7. Percent degradation of Phenol Red (PR) under Solar radiations as a function of time (initial concentration of PR = 50 mg L^{-1}; Photo-catalyst load= 150 mgL^{-1}).

Conclusion

Nano size nitrogen doped TiO_2 and TiO_2/WO_3 composite semiconductor powders were synthesized using sol-gel and hydrothermal techniques. Nitrogen doped TiO_2 exhibited higher degradation of phenol red dye under visible/solar radiation than under UV light due to lowering of band gap and thus enhanced photo absorption in the visible region of radiation. Nitrogen doping as well as compositing of WO_3 with TiO_2 showed synergetic effect towards improving the photo-catalytic degradation of phenol red in aqueous solution. With the dye initial concentration: 50 mg L^{-1} and N-doped TiO_2/WO_3 photo-catalyst load: 150 mgL^{-1} its degradation, as high as 92.6%, could be achieved within three hrs. Therefore, the above composite photo-catalyst can be recommended for a low cost and efficient treatment of bulk water or effluents contaminated with phenol red and the purified water thus obtained may be used for domestic and agriculture sectors.

Acknowledgement

The authors thank the Research and Extension Office of Haramaya University for providing the financial grant for the research (HURG-2014-03-03 and HURG-2016-03-02) and Project MAT2016-77496-R (AEI/FEDER, UE) from Spain for materials characterization.

References

1. Roldán MD, Blasco R, Caballero FJ, Castillo F (1997) Degradation of p-Nitrophenol by the Phototrophic Bacterium Rhodobacter capsulatus. Arch Microbiol 169: 36-42.

2. Anvari FH, Amirkolaie AK, Jalali AM, Miandare HK, Sayed AH, et al. (2018) Environmental Pollution and Toxic Substances; Cellular Apoposis as a Key Parameter in a Sensible Model Like Fish. Aquat Toxicol 204: 144-159.

3. Guesh K, Taddesse AM, Yadav OP (2014) Effect of Ag-N co-doping in Nanosize TiO_2 on Photo-catalytic Degradation of Methyl Orange Dye. J Surf. Sci Tech 29: 1-14.

4. Yadav M, Ali S, Yadav OP (2015) Photo-catalytic Degradation of Victoria Blue-B Dye Using ZnS and ZnS/Fe_2O_3 Composite Nanoparticles Under Visible Radiation. Der Chemica Sinica 6: 28-37.

5. Elizondo GP, Hernandez-Ramirez A (2017) Photo-catalytic Degradation of Ibuprofen Using TiO_2 Sensitized by Ru(II) Polyaza Complexes. Photochem. Photobiol Sci 16: 31-37.

6. Ani IJ, Akpan UG, Olutoye MA Hameed BH (2018) Photo-catalytic Degradation of Pollutants in Petroleum Refinery Wastewater by TiO2- and ZnO-based Photo catalysts: Recent Development. J Cleaner Production 205: 930-954.

7. Kakhki RM, Hedayat S, Mohammadzadeh K (2019) Novel, Green and Low Cost Synthesis of Ag Nanoparticles with Superior Adsorption and Solar Based Photo- catalytic activity. J Mater Sci Materials in Electronics 30: 8788-8795.

8. Bharkhnade DS, Pangarkar VG, Beenackers AACM (2002) Photo-catalytic Degradation for Environmental Applications-A Review. J Chem Technol Biotechnol 77: 102-116.

9. Pawar M, Sendoğdular ST, Gouma P (2018) A Brief Overview of TiO_2 Photocatalyst for Organic Dye Remediation: Case Study of Reaction Mechanisms Involved in Ce-TiO_2 Photo-catalysts System. J Nanomaterials Article ID 5953609.

10. In S, Orlov A, Berg R, García F, Jimenez SP, et al. (2007) Effective Visible Light-activated B-doped and B, N-co-doped TiO_2 Photo-catalysts. J Amer Chem Soc 129: 13790-13791.

11. Xie J, Jiang D, Chen M, Li D, Zhu J, et al. (2010) Preparation and Characterization of Monodisperse Ce-doped TiO_2 Microspheres with Visible Light photocatalytic Activity. Colloids and Surfaces A: Physicochem. Eng. Aspects 372: 107-114.

12. Reza KM, Kurny ASW, Gulshan F (2017) Parameters Affecting Photocatalytic Degradation of Dyes Using TiO_2-A Review. Appl Water Sci 7: 1569-1578.

13. Kim S, Choi W (2005) Visible-Light-Induced Photo-catalytic Degradation of 4- Chlorophenol and Phenolic Compounds in Aqueous Suspension of Pure Titania: Demonstrating the Existence of a Surface-Complex-Mediated Path. J Phys Chem B 109: 5143-5149.

14. Ihara T, Miyoshi M, Iriyama Y, Matsumoto O, Sugihara S (2003) Visible –Light- Active Titanium Oxide Photo-catalyst Realized by an Oxygen-deficient Structure and by Nitrogen Doping. Applied Catalysis B 42: 403-409.

15. Welderfael T, Yadav OP, Taddesse AM, Kaushal J (2013) Synthesis, Characterization and Photo-catalytic Activities of Ag-N-codoped ZnO nanoparticles for Degradation of Methyl Red. Bull Chem Soc Ethiop 27: 221-232.

16. Nibret A, Yadav OP, Diaz I, Taddesse AM (2015) Cr-N co-doped ZnO Nanoparticles: Synthesis, Characterization and Photo-catalytic Activity for degradation of Thymol Blue. Bull Chem Soc Ethiop 29: 247-258.

17. Balcha A, Yadav OP, Dey T (2016) Photo-catalytic Degradation of Methylene Blue Dye by ZnO Nanoparticles obtained from Precipitation and Sol-gel Methods. Environ Sci Pollut Res 23: 25485-25493.

18. Dagme Z, Yadav OP, Taddesse AM (2017) Photo-catalytic Degradation of Methylene Blue Dye in Water Over Mn-N co-doped ZnS Nanoparticles. Current Phys Chem 7: 1-9.

19. Bargole S, George S, Saharan VK, Pandit, AB (2019) Synthesis and Characterization of Samarium and Nitrogen doped TiO2 Photo-catalysts for Photo-degradation of 4-acetamidophenol in Combination with Hydrodynamic and Acoustic Cavitation. Separat Purif Technol 209: 254-269.

20. Sant PA, Kamat PV (2002) Interparticle Electron Transfer Between Size-quantized CdS and TiO_2 Semiconductor Nanoclusters. Phys Chem Chem Phys 4: 198-2003.

21. Tian J, Sang Y, Zhao Z, Zhou W, Wange D, et al. (2013) Enhanced Photo-catalytic Performances of CeO_2/TiO_2 Nanobelt Heterostructures Small 9: 3864-3872.

22. Kwon YT, Song KY, Lee WI, Choi GJ, Do YR (2000) Photo-catalytic Behavior of WO3-Loaded TiO_2 in an Oxidation Reaction. J Catal 191: 192-199.

23. Song KY, Park MK, Kwon YT, Lee HW, Chung WJ, et al. (2001) Preparation of Transparent Particulate MoO_3/TiO_2 and WO_3/TiO_2 and Their Photo-catalytic Properties. Chem Mater 13: 2349-2355.

24. Boga B, Szekely I, Pap Z, Baia L, Baia M (2018) Detailed Spectroscopic and Structural Analysis of TiO_2/WO_3 Composite. Semiconductors. J Spectr Article ID 6260458.

25. Bessekhouad Y, Robert D, Weber JV (2003) Preparation of TiO_2 Nanoparticles by Sol-Gel route. Intern J Photoenergy 5: 153-158.

26. Wawrzyniak B, Morawski AW, Tryba B (2006) Preparation of TiO_2-Nitrogen-Doped Photocatalyst Active under Visible Light. Inter J of Photoenergy 23: 1-8.

27. Ren G, Gao Y, Yin J, Xing A, Liu H (2011) Synthesis of High-Activity TiO_2/WO_3 Photo-catalyst via Environmentally Friendly and Microwave Assisted Hydrothermal Process. J Chem Soc Pak 33: 666-670.

28. Achamo T, Yadav OP (2016) Removal of 4-Nitrophenol from Water Using Ag-N-P Tridoped TiO_2 by Photo-catalytic Oxidation Technique. Anal Chem Insight 11: 29:34.

29. Huang BS, Chang FY, Wey MY (2010) An Efficient Composite Growing N-doped TiO_2 on Multi-Walled Carbon Nanotubes Through Sol–gel Process. J Nanoparticle Res 12: 2503-2510.

30. Grigioni I, Stamplecoskie KG, Jara DH, Dozzi MV, Oriana A, et al. (2017) Wavelength-dependent Ultrafast Charge Carrier Separation in the WO_3/$BiVO_4$ Coupled system. ACS Energy Letters 2: 1362-1367.